



Khan, I.U., Javaid, N., Taylor, C.J., Gamage, K.A.A. and Ma, X. (2020) Optimal Power Flow Solution with Uncertain RES using Augmented Grey Wolf Optimization. In: 2020 IEEE International Conference on Power System Technology (POWERCON 2020), 14-16 Sept 2020, ISBN 9781728163512 (doi:[10.1109/POWERCON48463.2020.9230659](https://doi.org/10.1109/POWERCON48463.2020.9230659))

The material cannot be used for any other purpose without further permission of the publisher and is for private use only.

There may be differences between this version and the published version. You are advised to consult the publisher's version if you wish to cite from it.

<http://eprints.gla.ac.uk/223504/>

Deposited on 29 September 2020

Enlighten – Research publications by members of the University of
Glasgow
<http://eprints.gla.ac.uk>

Optimal Power Flow Solution with Uncertain RES using Augmented Grey Wolf Optimization

Inam Ullah Khan^{1,*}, Nadeem Javaid², C. James Taylor¹, Kelum A. A Gamage³ and Xiandong MA¹

¹Engineering Department, Lancaster University, Bailrigg, Lancaster LA1 4YW, UK

²Department of Computer Science, COMSATS University Islamabad, Islamabad, 44000, Pakistan

³School of Engineering, University of Glasgow, Glasgow G12 8QQ, UK

*Correspondence: i.u.khan@lancaster.ac.uk

Abstract—This work primarily focuses on an implementation of the optimal power flow (OPF) problem, considering wind, solar and hydro power generation. The stochastic nature of renewable energy sources (RES) is modelled using lognormal, Weibull and Gumbel probability density functions. The system wide economic aspect is examined with additional cost functions such as penalty and reserve costs for under and overestimation of RES power outputs imbalance. Also, a carbon tax is imposed on carbon emissions as a separate objective function to enhance the green energy contribution. For solving the optimization problem, augmented grey wolf optimization is employed and tested on IEEE-30, 57 and 118 bus systems. The simulation results obtained using the proposed method are compared with other state of the art methods available in the literature for a case of OPF incorporating RES. Subsequently, an extensive simulation study is conducted to investigate the effect of different cost functions on optimal dispatch and emission. Numerical simulations indicate that the proposed method has better exploration and exploitation capabilities to reduce operational costs and carbon emissions.

Index Terms—Optimal power flow, Renewable energy sources, Carbon emission, Meta-heuristic techniques, Grey wolf optimization.

I. INTRODUCTION

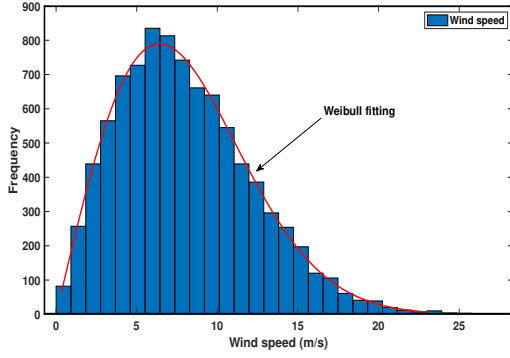
Since its inception, optimal power flow (OPF) has proved to be an important tool for efficient and secure operation of power networks. The main objective of OPF is to find optimal settings of the control variables with certain objective functions while satisfying system equality and inequality points. The system control variables that need adjustment include generated active power, the voltage of all generation buses and tap settings of transformer. During the optimization process, system constraints such as transmission line capacity, power flow balance, voltage profile of all buses and generator capability constraint need to be maintained. To solve the OPF problem, several classical (deterministic) and modern (nondeterministic) heuristic methods have been proposed. However, classical methods are usually trapped in local optimal solution due to nonlinear and multimodal optimization characteristics in OPF problem. To solve this problem, metaheuristic optimization techniques are proposed which are good to find global optimal solution for OPF problem.

OPF with only traditional thermal power generators (TPGs) is widely studied in the literature. A recent work proposed in [1] described the application of differential search algorithm to optimize few objectives for a standard IEEE-30 bus system.

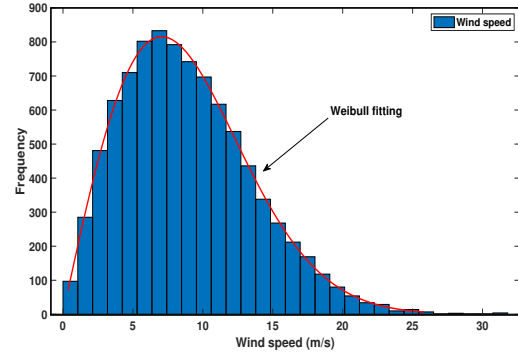
With improved search capabilities, authors in [2] attempted the same optimization problem by employing a modified group search optimization algorithm. The authors in [3] proposed the backtracking search algorithm (BSA) for the OPF solution. This BSA was tested for multiple cases with complex objective functions based on valve point loading effect in TPGs. Particle swarm optimization (PSO) technique is used for solving the OPF problem in [4]. Most recently, a moth swarm algorithm (MSA) is applied in [5] on multiple objective problems of OPF problem. The algorithm is tested on different bus systems to show the effectiveness of the proposed technique in terms of quick convergence and fast execution time. It is important to note that all the aforementioned literature deals only with traditional TPGs. With increased penetration of RES, it is necessary to incorporate associated uncertainty into the power network.

Systems that consider both TPGs and RES are under recent studies in pursuit of similar objective functions studied in the past. In literature [4]–[8], extensive study has been conducted on the over/under estimation of wind power generation (WPG) in classical economic dispatch model. In all these studies, the Weibull probability distribution function is used to model the uncertainty of wind generator output. For economic dispatch strategies, these studies provide a valuable insight with wind integrated system. However, the challenge of wind speed variation on optimal dispatch schedule of power plants remain unaddressed. Also, reactive power capability of the wind power generators (WPGs), bus voltage constraints and loading effect of transmission line were not considered in the study.

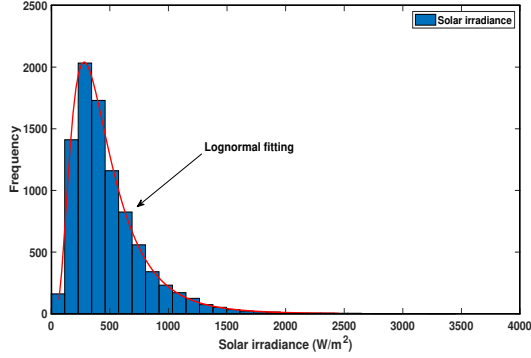
Authors in [9] combined advanced variant of differential evolution with an effective constraint handling technique for system that consider both solar and wind power generation in OPF problem. The uncertain and intermittent nature of both RES were modelled with lognormal and Weibull probability density functions (PDFs). However, the resulting algorithms sometimes attains premature convergence (i.e. becomes trapped in a local solution) and the convergence rate can be very slow. Furthermore, the scalability and robustness of the proposed algorithm was not verified since the algorithm was only verified on IEEE-30 bus system. This does not guarantee good performance over medium and higher bus systems (IEEE-57 and IEEE-118). In general, OPF with incorporation of RES needs further attention.



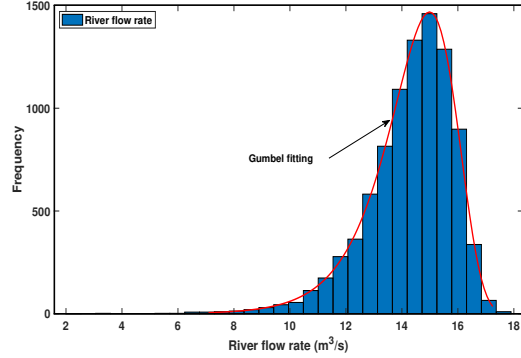
(a) Distribution of Wind Speed for Wind Farm 1 at Bus-5.



(b) Distribution of Wind Speed for Wind Farm 2 at Bus-11.



(c) Solar Irradiance Distribution for SPG at Bus-13.



(d) Hydro PDF Distribution at Bus-13.

Fig. 1: Probability Distribution Functions for Solar, Wind and Hydro Power Generations.

II. MATHEMATICAL MODEL

In this paper, IEEE-30, 57 and 118 bus standard test systems are used to validate proposed AGWO algorithms in the OPF problem. The essential characteristics of these bus test systems are shown in Table I. Along with the TPGs, RES such as wind, solar and small hydro (WSH) generators are selected as power generation sources for OPF framework. The power output from RES is variable in nature. This instability in power outputs needs to be minimized and balanced by the aggregation of the power outputs of all the generators and spinning reserve. Thus, total power generation cost is the combination of operating cost of all generators, reserve and penalty cost (due to the intermittent nature of power generation from RES). In subsequent sections, cost models are discussed in detail.

A. Stochastic Wind Power

The behaviour of the wind speed $v(m/s)$ distribution can be modelled with the help of Weibull PDF $f_v(v)$ by adjusting scale parameter c and shape parameter k as established by [4] and [7]. The probability of wind speed can be calculated by making use of the following equation:

$$f_v(v) = \frac{k}{c} \left(\frac{v}{c}\right)^{k-1} \exp \left[-\left(\frac{v}{c}\right)^k \right], \quad 0 < v < \infty \quad (1)$$

In the modified IEEE-30 bus test system, TPGs at bus 5 and bus 11 are replaced with the WPGs. The values for scale c

and shape k parameters are given in Table III. The wind speed behavior for WPG 1 and WPG 2 at buses 5 and 11 follow the Weibull PDF, as shown in Figs. 1a and 1b, respectively.

In this paper, we consider wind power output at bus five as the total power generated from 25 turbines and wind power output at bus 11 as the cumulative output of the 20 wind turbines. Each turbine has rated the power of 3 MW. The actual power output from wind turbines is entirely dependent on the wind speed. The relationship between wind speed and actual power extracted from wind turbine given in Eq. 2 [7]:

$$P_W = \begin{cases} 0, & v < v_{ci} \text{ or } v > v_{co} \\ P_{Wr}, & v_r < v \leq v_{co} \\ P_{Wr} \left(\frac{v-v_{ci}}{v_r-v_{ci}} \right)^3, & v_{ci} \leq v \leq v_r, \end{cases} \quad (2)$$

where v , v_{ci} , v_{co} , v_r and P_{Wr} represent the forecasted, cut-in, cut-off, rated wind speed and rated output power of the WPG, respectively. The wind speed values for v_{ci} , v_{co} and v_r are 3 m/s, 25 m/s and 16 m/s, respectively.

B. Stochastic Solar Power

Similarly, the TPG at bus 13 of the modified IEEE-30 bus system is replaced with the solar power generator (SPG). The output power from SPG depends upon the solar irradiance

which follows lognormal PDF. The probability with standard deviation λ and mean σ can be calculated as [4]:

$$f_X(X) = \frac{1}{X\sigma\sqrt{2\pi}} \exp\left\{-\frac{[\ln X - \lambda]^2}{2\sigma^2}\right\}, \quad X > 0 \quad (3)$$

Based on the lognormal PDF, SPG irradiance behavior at bus 13 is shown in Fig. 1c. Also, the values for lognormal parameters λ and σ are given in Table III. The relationship between the solar irradiance X (W/m^2) and the power produced from the SPG can be calculated in the following equation:

$$P_S(X) = \begin{cases} P_{SR}\left(\frac{X^2}{X_{std}C_I}\right), & 0 < X < C_I \\ P_{SR}\left(\frac{X}{X_{std}}\right), & X > C_I, \end{cases} \quad (4)$$

where X , X_{std} , C_I and P_{SR} are the forecasted solar irradiance, solar irradiance value ($800 W/m^2$) in the standard environment, certain irradiance point ($120W/m^2$) and rated power of the SPG, respectively.

C. Stochastic Hydro Power

The hydro power generator (HPG) output depends on the water flow rate (G_h) and pressure head (P_h). The water flow rate follows Gumbel PDF. The Gumbel PDF for water flow rate with scale parameter ω and location parameter γ can be mathematically formulated as [6]:

$$f_H(G_h) = \frac{1}{\omega} \exp\left[-\frac{(G_h - \omega)}{\omega}\right] \exp\left[-\exp\frac{(G_h - \omega)}{\omega}\right] \quad (5)$$

In the modified IEEE 30-bus system the TPG at bus number 13 is replaced with 45 MW SPG and 5 MW small HPG. The solar irradiance distribution and lognormal fitting available for SPG at bus 13 is shown in Fig. 1b, while Fig. 1c shows water flow rate frequency distribution and Gumbel fitting. Both these figures are obtained by simulating 9000 Monte Carlo scenarios. The values of all PDF parameters are realistically chosen and many of them are almost same as provided in Ref. [4]. The output hydropower as a function of water flow rate and pressure head can be described as:

$$P_h(G_h) = \alpha_{pg} G_h H_h \quad (6)$$

where, α is the efficiency of the generating unit and assumed as 0.85, β is the density of water volume and taken as 1000 kg/m³, g represents the value of gravitational acceleration, G_h is the water flow rate, and P_h is the pressure head of water across the turbine.

D. Cost Model for Thermal Power Generators

Thermal generator units require fossil fuel for their operation. The relationship between generated power (MW) and fuel cost (\$/h) can be calculated with the help of the quadratic equation:

$$C_T = \sum_{i=1}^{N_T} a_i + b_i P_{Ti} + c_i P_{Ti}^2 \quad (7)$$

Practically, the valve point loading effect needs to be considered to model accurate cost function. Hence, the overall thermal power generation cost (\$/h) becomes:

$$C_T = \sum_{i=1}^{N_T} a_i + b_i P_{Ti} + c_i P_{Ti}^2 + \left| d_i \times \sin\left(e_i \times (P_{Ti}^{min} - P_{Ti})\right) \right| \quad (8)$$

Where a_i , b_i and c_i are the coefficients of cost for the i -th thermal generator. P_{Ti} is the output power of i -th thermal generator. N_T signifies the total number of the TPGs. d_i and e_i represents the valve point loading effect coefficients. P_{Ti}^{min} signifies the minimum power produces by the i -th thermal generator. All emission and cost coefficients pertaining to thermal power generators (TPGs) are given in Table II.

E. Cost Model for Renewable Energy Sources

It is very challenging to integrate all RES into the grid due to their intermittent and uncertain nature. The total cost of the RES thus consists of direct cost associated with scheduled power, penalty cost for underestimation and reserve cost for overestimation.

For simplicity, the reserve and penalty cost models are constructed in line with the concept presented in references [4] – [8]. The direct, reserve and penalty costs of WPG as a function of scheduled power is represented as:

$$C_{DW,j} = d_{w,j} P_{WS,j} \quad (9)$$

$$C_{RW,j} = r_{w,j} \int_0^{P_{WS,j}} (P_{WS,j} - W) f_w(W) dW \quad (10)$$

$$C_{PW,j} = p_{w,j} \int_{P_{WS,j}}^{P_{WR,j}} (W - P_{WS,j}) f_w(W) dW \quad (11)$$

where, $d_{w,j}$, $r_{w,j}$ and $p_{w,j}$ are direct, reserve and penalty cost coefficients pertaining to j -th WPG. $P_{WS,j}$ is the scheduled power and $f_w(W)$ is probability density function of same wind power generator (WPG).

With the help of Eqs. 3–6, the total cost of WPG can be calculates as:

$$C_{TW,j} = C_{DW,j} + C_{RW,j} + C_{PW,j} \quad (12)$$

Likewise, the SPG also has uncertain power output. The direct, reserve and penalty costs pertaining to the k -th SPG are represented as:

$$C_{DS,k} = d_{s,k} P_{SS,k} \quad (13)$$

$$C_{RS,k} = r_{s,k} \cdot Pr(P_{AS,k} < P_{SS,k}) \cdot [(P_{SS,k} - E(P_{AS,k} < P_{SS,k}))] \quad (14)$$

$$C_{PS,k} = p_{s,k} \cdot Pr(P_{AS,k} > P_{SS,k}) \cdot [(E(P_{AS,k} > P_{SS,k}) - P_{SS,k}] \quad (15)$$

TABLE I: Characteristics of Bus Systems Under Consideration

Items	IEEE-30 Bus System		IEEE-57 Bus System		IEEE-118 Bus System	
	Quantity	Details	Quantity	Details	Quantity	Details
Number of buses	30	[4]	57	[3]	118	[5]
Number of Branches	41	[4]	80	[3]	186	[5]
Number of TPGs	3	Connect at bus 1 (Swing), 2 and 8	7	Connect at bus 1 (slack), 3, 8 and 12	54	1,4,6,8,10,12,15,18,19,24,25,26, 27, 31, 32, 34, 36, 40, 42, 46, 49, 54, 55, 56, 59,61, 62, 65, 66, 69 (Swing), 70, 72,73, 74, 76, 77, 80, 85, 87, 89, 90, 91, 92,99, 100,103, 104, 105, 107, 110, 111, 112,113, and 116.
Number of WPGs	2	Connect at bus 5 and 11	2	Connect at bus 2 and 6	2	Connect at bus 5 and 11
Number of SPGs	1	Connect at bus 13	1	Connect at bus 9	1	Connect at bus 9
Number of HPG	1	Connect at bus 11	1	Connect at bus 11	1	Connect at bus 11
Input variables	11	Scheduled power for five generators without P_{T1} (Slack bus) and bus voltages for all generator buses (with slack bus)	13	Scheduled power for seven generators without P_{T1} (Slack bus) and bus voltages for all generator buses (with slack bus)	15	Scheduled power for seven generators without P_{T1} (Slack bus) and bus voltages for all generator buses (with slack bus)
Connected load	—	283.4 MW, 126.2 MVar	—	1250.8 MW, 336.4.2 MVar	—	4242 MW, 1439 MVar
Control variables	24	—	33	—	120	—
Load Bus voltage range	24	[0.95-1.06] p.u.	50	[0.94-1.06] p.u.	64	[0.94-1.06] p.u.

TABLE II: Thermal Power Generators Cost and Emission Coefficients for the System [4].

Thermal generator	Bus number	a	b	c	d	e	f	g	h	k	l
TPG1	1	0	2	0.00375	18	0.037	4.091	-5.554	6.49	0.0002	6.667
TPG2	2	0	1.75	0.0175	16	0.038	2.543	-6.047	5.638	0.0005	3.333
TPG3	8	0	3.25	0.00834	12	0.045	5.326	-3.55	3.38	0.002	2

TABLE III: PDF Parameters for Wind, Solar and Hydro Power Generation [6]

Wind power generation plants				Solar + Hydro power generation plant (bus 13)			
Windfarm #	No. of wind turbines	Total rated power	Weibull PDF parameters	Rated power of SPG	Lognormal PDF parameters	Rated power of HPG	Gumbel PDF parameters
1 at bus 5	25	75 MW	$c = 9, k = 2$	45 MW	$\lambda = 6, \sigma = 0.6$	5 MW	$c = 4, d = 5$
2 at bus 11	20	60 MW	$c = 10, k = 2$				

In Eqs. 13–15, $d_{s,k}$, $r_{s,k}$ and $p_{s,k}$ are direct, reserve and penalty cost coefficients pertaining to k-th SPG. $P_{AS,k}$ and $P_{SS,k}$ represent available and scheduled power from SPG. The terms $E(P_{AS,k} < P_{SS,k})$ and $E(P_{AS,k} > P_{SS,k})$ represent expected power of SPG below and above the $P_{SS,k}$. Similarly, $Pr(P_{AS,k} < P_{SS,k})$ and $Pr(P_{AS,k} > P_{SS,k})$ are the occurrence probabilities of the available SPG less and above $P_{SS,k}$. Finally, the total cost of SPG can be calculated as:

$$C_{TS,k} = C_{DS,k} + C_{RS,k} + C_{PS,k} \quad (16)$$

As a third RES, we consider a small-hydro power generator (HPG) in this study. The output of HPG is very less (10–20 % of total install capacity) so, it is combined with WPG owned by a single private operator. Stochastic power output from the combined system is computed in section 3. The direct cost coefficients of both these units are different. However, scheduled output power agreed by distribution system operator (DSO) is a fixed amount and this power is delivered jointly by the WPG and small-HPG unit. Following Eqs 13–15, direct, reserve cost for overestimation and penalty cot for

underestimation of combined generation system of solar hydro power is:

$$C_{SH} = d_s P_{SSH,s} + d_h P_{SSH,h} \quad (17)$$

$$C_{RSH} = r_{sh,m} \cdot Pr(P_{ASH} < P_{SSH}) \cdot [(P_{SSH} - E(P_{ASH} < P_{SSH}))] \quad (18)$$

$$C_{PSH} = p_{sh,m} \cdot Pr(P_{ASH} > P_{SSH}) \cdot [(E(P_{ASH} > P_{SSH}) - P_{SSH})] \quad (19)$$

where, $P_{SSH,s}$ and $P_{SSH,h}$ represent scheduled power from SPG and HPG, respectively. d_h , r_{sh} and p_{sh} are direct, reserve and penalty cost coefficients pertaining to m-th HPG. P_{ASH} and P_{SSH} represent available and scheduled output power from combined solar hydro power generator. Finally, the total cost of HPG can be calculated as:

$$C_{TSH} = C_{DSH} + C_{RSH} + C_{PSH} \quad (20)$$

F. Carbon Tax based Emission Model

Unlike RES, producing power from TPGs emits the harmful gases such as, CO_x , NO_x and SO_x into the environment. The increment in generated power from TPGs is directly proportional to the harmful gases emission. Emission E (tonne/h) is calculated with the following equation:

$$F_C = \sum_{i=1}^{N_T} [(a_i + b_i P_{T_i} + c_i P_{T_i}^2) \times 0.01 + d_i e^{l_i P_{T_i}}] \quad (21)$$

where a_i , b_i , c_i , d_i and l_i are the emission coefficients related to i -th TPG.

The combustion fossil fuels on which TPGs run is the main source of greenhouse gases (GHGs) emission. The emission of GHGs results in gradual heating of the earth's atmosphere and surface. To control GHGs and make clean energy economy, the carbon tax is levied in many countries on per unit emission of the carbon amount [4]. The carbon emission tax (emission cost) can be modelled as follows:

$$C_E = E \cdot C_{tax} \quad (22)$$

where C_E is the emission cost and C_{tax} represents the carbon tax per unit of carbon emission.

III. PROBLEM FORMULATION

The main objective of the OPF problem is formulated by incorporating all the cost functions described in the above sections. The first objective F_1 of the optimization problem is to minimize the total generation cost. However, emission cost is not included in its formulation. To analyze the impact of carbon tax on generation scheduling, the second objective F_2 is modelled by adding the carbon emission cost with the first objective.

The objective is as follows: minimize

$$F_1 = \sum_{i=1}^{N_T} C_{TG} + \sum_{j=1}^{N_W} C_{TW} + \sum_{k=1}^{N_S} C_{TS} + \sum_{m=1}^{N_{SH}} C_{TSH} \quad (23)$$

where N_{Wg} , N_{Sg} and N_{SHg} are the numbers of wind, solar and combined solar hydro generators in the system. The second objective F_2 of the optimization is:

$$\text{Minimize } F_2 = F_1 + C_E \quad (24)$$

where C_E is the emission cost, calculated in Eq. 22.

Both OPF objective functions, Eqs. 23 and 24, are subject to system equality and inequality constraints. Equality constraints are used for power balancing of both real and reactive power generated to the total demand and losses in the system. Whereas, inequality constraints comprise of the operating limits imposed on the component and equipment installed in the power network.

IV. THE GREY WOLF OPTIMIZATION ALGORITHM

GWO was proposed by Mirjalili et al. 2014 [11] and it is inspired by the leadership and hunting behaviour of grey wolves which live in the form of a pack. In GWO, wolves are categorised into four different levels: alpha (α), beta (β), delta (δ) and omega (ω) wolves. From the top to bottom of the leadership hierarchy, α wolves are known to be the superior. Their role is decision making in the pack. Alpha wolves are followed by β wolves, whose role is to help α wolves in decision making and to carry out other important activities in the pack.

In regard to GWO, accurate determination of prey location is treated as the optimization problem (fittest solution), while the position of the wolves relative to the prey determines the best solution. The position of the α wolves is said to be the best solution found so far in the search space, because they are expected to be closer to the prey than other wolves in the pack. To allocate their position in the search space, these wolves are represented as X_α , X_β and X_δ . Fourth level ω wolves update their position X_ω in accordance with the relative position of the α , β and δ wolves. Finally, hunting for prey is achieved by adopting four main steps, namely encircling, hunting, attacking and searching again.

The process of hunting a prey by grey wolves is: searching for the prey, encircling the prey, then hunting and attacking the prey. The mathematical model of encircling the prey is expressed as follows:

$$\vec{X}(t+1) = \vec{X}_p(t) - \vec{A} \times \vec{D} \quad \text{where, } \vec{D} = |\vec{C} \times \vec{X}_p(t) - \vec{X}(t)| \quad (25)$$

and t indicates the current iteration, while $\vec{X}(t)$ and $\vec{X}_p(t)$ are position vectors representing the current location of the grey wolf and prey in the search space, respectively. The coefficient vectors \vec{A} and \vec{C} are determined as follows:

$$\vec{A} = 2\vec{a} \times \vec{r}_1 - \vec{a} \quad \text{and} \quad \vec{C} = 2 \times \vec{r}_2 \quad (26)$$

To control exploration and exploitation, the components of \vec{a} are linearly decreased from 2 to 0 over the course of an iteration. Note that \vec{r}_1 and \vec{r}_2 are random vectors whose values are chosen between [0, 1]. To reach prey position (X_p, Y_p), the current position of a grey wolf (X, Y) is updated with Eqs. 25–26. The value of \vec{a} is assumed the same for all the wolves in a population. A wolf can update its position according to the best agent in different places by setting the values of \vec{C} and \vec{A} .

After finding the prey location, the grey wolves encircle it. The α wolves guide the pack for prey hunting, while β and δ wolves also contribute. Initially, the α , β and δ wolves location are saved as the 'best' location, representing their better knowledge to recognise prey location. The remaining search agents, mainly ω wolves, update their location in accordance with the position of the best search agents. For α , β and δ wolves, position location is determined as follows:

$$\vec{D}_\alpha = |\vec{C}_1 \times \vec{X}_\alpha(t) - \vec{X}(t)|, \quad \vec{D}_\beta = |\vec{C}_2 \times \vec{X}_\beta(t) - \vec{X}(t)| \quad (27)$$

$$\vec{D}_\delta = | \vec{C}_3 \times \vec{X}_\delta(t) - \vec{X}(t) |, \quad \vec{X}_1 = | \vec{X}_\alpha - A_1 \times \vec{D}_\alpha | \quad (28)$$

$$\vec{X}_2 = | \vec{X}_\beta - A_2 \times \vec{D}_\beta |, \quad \vec{X}_3 = | \vec{X}_\delta - A_3 \times \vec{D}_\delta | \quad (29)$$

$$\vec{X}(t+1) = \frac{\vec{X}_1 + \vec{X}_2 + \vec{X}_3}{3} \quad (30)$$

At iteration t , the distance between $\vec{X}(t)$ and the three best hunt agents (\vec{X}_α), (\vec{X}_β) are (\vec{X}_δ) are determined using Eqs. 27–29, in which A_1 , A_2 and A_3 are random vectors as defined in Eq. 26. Finally, wolves movement towards prey is updated by Eq. 30.

VI. AUGMENTED GREY WOLF OPTIMIZATION ALGORITHM

For global optimization and wide-range application, the GWO algorithm is presented in its simplest structure. Therefore, similar to the other proposed algorithms (e.g. PSO), the GWO algorithm can be improved and modified for better performance of exploration and exploitation in different discipline applications. In this paper, a new modification is proposed to augment the exploration of the GWO algorithm without affecting its simplicity, flexibility, and global optimization. As described in the previous section, the most parameter responsible for exploration and exploitation is parameter A which mainly depends on parameter a as in Eq. 26. The behaviour of parameter a controls the exploration and exploitation of GWO algorithm, where parameter a change linearly from 2 to 0 in the original GWO algorithm. In the proposed augmentation (AGWO) algorithm, parameter a changes nonlinearly and randomly from 2 to 1 as in Eq. 31, where the chances of exploration state is more than exploitation [10].

$$\vec{a} = 2 - \cos(rand) \times t / Max_iter \quad (31)$$

$$\vec{A} = 2\vec{a} \times \vec{r}_1 - \vec{a}, \quad \vec{C} = 2 \times \vec{r}_2 \quad (32)$$

The hunting and decision-making in the GWO algorithm depends on the updating of alphas (α), betas (β) and deltas (δ) as in Eqs. 28 and 29. However, in the proposed AGWO algorithm the hunting will depends only on α betas (β) as in Eq. 33.

$$\vec{D}_\alpha = | \vec{C}_1 \times \vec{X}_\alpha(t) - \vec{X}(t) |, \quad \vec{D}_\beta = | \vec{C}_2 \times \vec{X}_\beta(t) - \vec{X}(t) | \quad (33)$$

$$\vec{X}_1 = | \vec{X}_\alpha - A_1 \times \vec{D}_\alpha |, \quad \vec{X}_2 = | \vec{X}_\beta - A_2 \times \vec{D}_\beta | \quad (34)$$

$$\vec{X}(t+1) = \frac{\vec{X}_1 + \vec{X}_2}{2} \quad (35)$$

VI. CASE STUDIES FOR IEEE-30 BUS SYSTEM

The IEEE-30 bus system is a small size power system with active and reactive power demand of 283.4 MW and 126.2 MVAR, respectively. The main characteristics of IEEE 30-bus system are summarized in Table I.

A. Case 1: Optimization of Total Generation Cost

The objective of Case-1 is to optimize the power generation schedule of all RES and TPG to reduce total power generation cost using Eq. 23. For this purpose, WPG direct cost coefficients are $d_{w,1} = 1.6$ and $d_{w,2} = 1.75$, respectively. Reserve and penalty cost coefficient values are similar to [3] i.e., $r_{w,1} = r_{w,2} = 3$ and penalty cost coefficients value are $p_{w,1} = p_{w,2} = 1.5$. Control variables optimum settings, reactive power of the generator (Q), total power generation cost, total power loss (total P_{loss}), carbon emission and total voltage deviation (VD) for all techniques are given in Table IV. The total generation cost achieved by AGWO is 782.1930 \$/h and that of GWO is 781.1317 \$/h shown in Table IV. These results are compared with the results obtained from SHADE-SF [?], i.e., 782.503 \$/h and ABC. Fig. 2a shows that AGWO has faster convergence compared to the other three algorithms.

B. Case 2: Optimizing Fuel Cost and Carbon Emission

The main objective of case 2 is to minimize total generation cost while imposing carbon tax on the amount of carbon emission from TPGs. Total generation cost, including the carbon tax, is calculated with the help of Eq. 24. Carbon tax (Ctx) is considered at the rate of 20/tonne [24]. The optimized generation schedule, reactive power, total power generation cost, including the carbon tax and other parameters for all three algorithms are provided in Table IV. It is clearly depicted that power generation cost gets higher from RES when the carbon tax is imposed in Case-2 as compared to Case-1 (when there is no tax on carbon emission). The obtained result of emission gases by AGWO is 0.20259 ton/h, which is the lowest value compared with 0.20503 ton/h, 0.20487 ton/h, 0.2049 ton/h, and 0.20486 ton/h obtained by GWO, ABC and SHADE-SF, respectively, as given in Table IV. The convergence characteristics of AGWO and other techniques are shown in Fig. 2b.

VII. CASE STUDIES FOR IEEE-57 BUS SYSTEM

To validate the performance of proposed AGWO algorithm on medium scale power system, the IEEE-57 bus system is used with active and reactive power demand of 1250.8 MW and 336.4 MVAR, respectively. The main characteristics of this bus system are provided in in Table I.

A. Case 3: Optimization of Total Generation Cost

The objective of Case-3 is to optimize the power generation schedule of three RES and TPGs to reduce total power generation cost in IEEE-57 bus system. It is similar to Case-1 in IEEE-30 bus system and the objective function of basic quadratic fuel cost is given in Eq. 23. Fuel cost obtained by AGWO algorithm is 21215 \$/h; this value is the best solution compared with those obtained by ABC, SHADE-SF, and GWO algorithms. The fuel cost value by ABC is 21262 \$/h, by SHADE-SF is 21260 \$/h and by the GWO is 21247 \$/h as given in Table V. The convergence characteristics of AGWO and the other optimization techniques are shown in Fig. 2c.

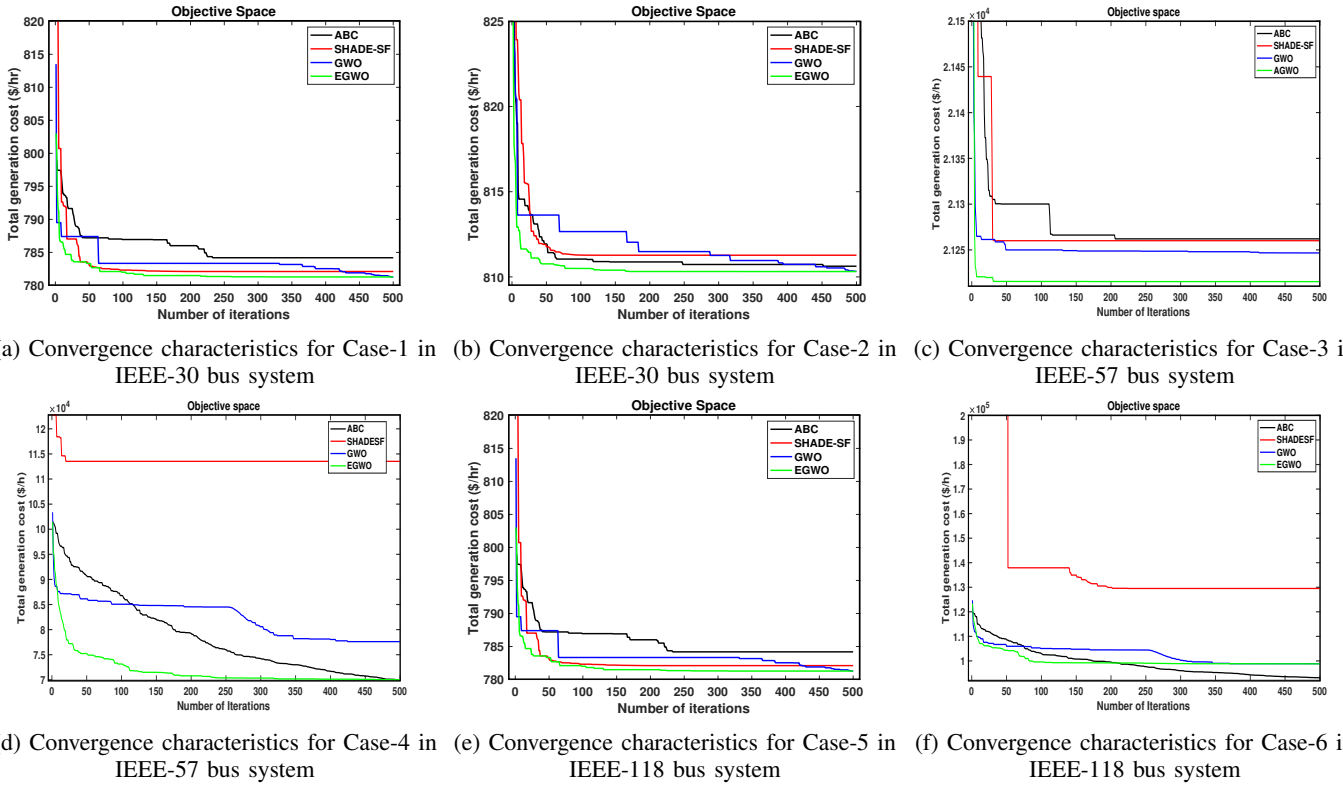


Fig. 2: Convergence Characteristics of Different Optimization Techniques for Case-1–Case-6.

TABLE IV: Comparison Between AGWO and other Algorithms for IEEE-30 bus System using Case-1 and Case-2.

			Case-I				Case-II			
	Min	Max	(ABC)	(SHADE-SF)	(GWO)	(AGWO) [10]	(ABC)	(SHADE-SF)	(GWO)	(AGWO)
$P_{Tg,1}$ (MW)	50	140	131.4	130.6	129.6	130.1	108.4	109.6	109.8	108.1
$P_{Tg,2}$ (MW)	20	80	38.5	37.6	38.1	36.2	43.7	44.7	44.7	41.3
$P_{Wg,1}$ (MW)	0	75	37.5	43.8	48.9	39.5	42.8	43.5	42.4	41.7
$P_{Tg,3}$ (MW)	10	35	10.4	10	10	10	12.1	10.5	11.05	16.3
$P_{Wg,2}$ (MW)	0	60	39.8	40.0	37.8	40.1	44.0	43.9	43.9	43.7
P_{Sg} (MW)	0	50	31.2	31.9	31.9	32.8	36.9	35.7	36	36.3
V_1 (p.u.)	0.95	1.1	1.02	1.05	1.04	1.07	1.06	1.1	1.03	1.09
V_2 (p.u.)	0.95	1.1	1.01	0.95	0.90	1.05	1.03	1.08		
V_5 (p.u.)	0.95	1.1	1.02	1.00	0.9	1.03	1.01	1.07	1.08	1.09
V_8 (p.u.)	0.95	1.1	1.00	1.03	1.00	1.05	1.04	1.09	1.00	1.03
V_{11} (p.u.)	0.95	1.1	1.03	0.95	1.01	1.09	1.09	1.1	1.01	1.06
V_{13} (p.u.)	0.95	1.1	1.05	1.01	1.04	1.04	1.01	1.09	1.08	134.9
$P_{Tq,1}$ (MVar)	-20	150	-5.3	-2.6	-14.2	-12.24	6.6	-3.5	-10.9	-4.9
$P_{Tq,2}$ (MVar)	-20	60	15.5	12.2	12.8	24.9	9.1	11.9	21.6	8.59
$P_{Wq,1}$ (MVar)	-30	35	21.0	23.1	35	24.4	23.4	23.3	19.4	25.1
$P_{Tq,3}$ (MVar)	-15	40	39.9	40	40	40	40	35	40	40
$P_{Wq,2}$ (MVar)	-25	30	20.0	30	18.6	17.3	19.6	30	19.1	18.7
P_{Sg} (MVar)	-20	25	22.5	14.9	20.9	18.9	12.75	17.5	21.8	22.91
Total cost (\$/hr)			787.84	785.82	784.77	782.30	783.81	774.4	773	774.1
Elapsed time (Seconds)			367	272	279	368	395	272	286	289
Total P_l (MW)			5.6	5.8	6.47	5.75	4.6	4.6	4.6	4.5
Carbon emission (ton/hr)			1.42	1.35	1.2	1.80	0.7	0.42	0.42	0.39
Carbon tax (\$/hr)			-	-	-	-	-	-	-	-
V_d (p.u.)			1.0	0.4	0.85	0.45	0.56	1.08	1.08	1.11

B. Case 4: Optimizing Fuel Cost and Carbon Emission

The aim of this case is to find the OPF solution based on the minimum quadratic fuel cost and carbon emission. The objective function of this case is given in Eq. 23. The

obtained results of fuel cost and emission gases by AGWO are 21448 \$/h and 9.42 ton/h, respectively. These are the lowest values compared to GWO, SHADE-SF and ABC algorithms, where the fuel cost by GWO, SHADE-SF and ABC is 21449 \$/h, 22852 \$/h, and 21602 \$/h, respectively,

TABLE V: Simulation Results for IEEE-57 Bus system using Case-3 and Case-4.

Bus System	IEEE-57							
	ABC		SHADE-SF		GWO		AGWO	
	Case-3	Case-4	Case-3	Case-4	Case-3	Case-4	Case-3	Case-4
Objective function								
Cost (MW/h)	21262	21602	21260	22852	21247	21449	21215	21448
Carbon emission (ton/h)	33	16	39	23	47	10	31	9.42
Computational time (Sec)	470	448	330	298	220	253	247	255

TABLE VI: Simulation results for IEEE-118 Bus System using Case-5 and Case-6.

Bus System	IEEE-118							
	ABC		SHADE-SF		GWO		AGWO	
	Case-5	Case-6	Case-5	Case-6	Case-5	Case-6	Case-5	Case-6
Objective function								
Cost (MW/h)	69934	93119	113523	129509	77606	98869	70014	98803
Carbon emission (ton/h)	128	92	133	99	101	84	144	99
Computational time (Sec)	6319	7700	992	992	1906	3679	2377	2200

while the carbon emission values are 10 ton/h, 23 ton/h, and 16 ton/h, respectively. The convergence characteristics of AGWO and the other techniques are shown in Fig. 2d.

VIII. CASE STUDIES FOR IEEE-118 BUS SYSTEM

To validate the performance of proposed AGWO algorithm on medium scale power system, the IEEE-118 bus system is used with active and reactive power demand of 4224 MW and 1439 MVAR, respectively. The main characteristics of this bus system are provided in in Table I.

A. Case 5: Optimization of Total Generation Cost

The total fuel cost minimization of the generation system is taken as the basic case in this work. Calculation of this case is based on the objective function given in Eq. 23. The obtained fuel cost by AGWO is 70014 \$/h; this is the second lowest value compared with other techniques, where the fuel cost values obtained by GWO, SHADE-SF, and ABC algorithms are 77606 \$/h, 129509 \$/h, and 69934 \$/h, respectively, as given in Table IV. Comparison between the convergence characteristics of AGWO and other techniques reveals that the AGWO has the best performance as shown in Fig. 2e.

B. Case 6: Optimizing Fuel Cost and Carbon Emission

The aim of this case is to minimize both quadratic fuel cost and emission gases. Multi-objective function of this case is given in Eq. 24. The value of emission is reduced from 144 ton/h in Case 5 to 99 ton/h. The convergence characteristics of AGWO and the other techniques are shown in Fig. 2f.

IX. CONCLUSION

This paper presents a solution strategy for optimal power flow study considering intermittent nature of renewable energy sources (RES) and traditional TPGs in the system. The intermittency of the RES is modeled using different PDFs. The optimization problems are solved using recently developed augmented grey wolf optimization (AGWO) algorithm. The simulation results are obtained for IEEE-30, 57 and 118 bus systems. Moreover, the optimal scheduling of TPGs and WSH system is compared with state of the art algorithms for similar OPF framework. From simulation results, it is found that the proposed method based on AGWO algorithm gives better

accuracy of results compared to other well established methods tried in the past with faster convergence and better solution quality. Finally the optimal power flow study considering stochastic wind power shows that the optimal value of wind power from a particular wind farm not only depends on the values of the reserve and penalty cost coefficients associated with the wind farms but also on its location in power network as the transmission system capacity can limit wind power injection.

Acknowledgements The authors acknowledge funding support from COMSATS University Islamabad, Lahore campus and Lancaster University UK to support this project.

REFERENCES

- [1] Cain, Mary B., Richard P. O'Neill and Anya Castillo. "History of optimal power flow and formulations." Federal Energy Regulatory Commission (2012): 1-36.
- [2] Abaci, Kadir and Volkan Yamacli. "Differential search algorithm for solving multi-objective optimal power flow problem." International Journal of Electrical Power & Energy Systems 79 (2016): 1-10.
- [3] Taher, Mahrous A., et al. "Modified grasshopper optimization framework for optimal power flow solution." Electrical Engineering 101.1 (2019): 121-148.
- [4] Biswas, Partha P., P. N. Suganthan, and Gehan AJ Amaratunga. "Optimal power flow solutions incorporating stochastic wind and solar power." Energy Conversion and Management 148 (2017): 1194-1207.
- [5] Mohamed, Al-Attar Ali, Yahia S. Mohamed, Ahmed AM El-Gaafary and Ashraf M. Hemeida. "Optimal power flow using moth swarm algorithm." Electric Power Systems Research 142 (2017): 190-206.
- [6] Biswas, Partha P., et al. "Multiobjective economic-environmental power dispatch with stochastic wind-solar-small hydro power." Energy 150 (2018): 1039-1057.
- [7] Reddy, S. Surender, P. R. Bijwe, and Abhijit R. Abhyankar. "Real-time economic dispatch considering renewable power generation variability and uncertainty over scheduling period." IEEE Systems journal 9.4 (2014): 1440-1451.
- [8] Roy, Ranjit and H. T. Jadhav. "Optimal power flow solution of power system incorporating stochastic wind power using Gbest guided artificial bee colony algorithm." International Journal of Electrical Power & Energy Systems 64 (2015): 562-578.
- [9] Mirjalili, Seyedali, Seyed Mohammad Mirjalili, and Andrew Lewis. "Grey wolf optimizer." Advances in engineering software 69 (2014): 46-61.
- [10] Qais, Mohammed H., Hany M. Hasanien, and Saad Alghuwainem. "Augmented grey wolf optimizer for grid-connected PMSG-based wind energy conversion systems." Applied Soft Computing 69 (2018): 504-515.
- [11] Reddy, S. Surender and James A. Momoh. "Realistic and transparent optimum scheduling strategy for hybrid power system." IEEE Transactions on Smart Grid 6, no. 6 (2015): 3114-3125.